PROCEEDINGS A

royalsocietypublishing.org/journal/rspa

Research

Cite this article: Marro M, Leckert J, Rollier E, Salizzoni P, Bailly C. 2023 Wind tunnel evaluation of novel drafting formations for an elite marathon runner. *Proc. R. Soc. A* **479**: 20220836.
https://doi.org/10.1098/rspa.2022.0836

Received: 14 December 2022
Accepted: 14 July 2023

Subject Areas:
fluid mechanics

Keywords:
air resistance, drafting, marginal gain, running aerodynamics, wind tunnel experiments

Author for correspondence:
Massimo Marro
e-mail: marro.massimo@ec-lyon.fr

Wind tunnel evaluation of novel drafting formations for an elite marathon runner

Massimo Marro[1], Jack Leckert[1], Ethan Rollier[1], Pietro Salizzoni[1,2] and Christophe Bailly[1]

[1]Univ Lyon, CNRS, Ecole Centrale de Lyon, INSA Lyon, Univ Claude Bernard Lyon 1, LMFA, UMR5509, 36 Av. Guy de Collongue, Ecully 69130, France
[2]Department of Environmental, Land, and Infrastructure Engineering, Politecnico di Torino, Corso Duca degli Abruzzi 24, 10129 Turin, Italy

MM, 0000-0002-6661-9637

Drafting is a strategy in marathon running races that reduces the drag force acting on a designated runner. Drafting involves a formation of athletes, called pacers, running in front of (and sometimes behind) the designated runner. The present experiments evaluated complex formations involving up to seven pacers with the aim of enhancing the performances of an elite marathoner. Wind tunnel measurements with 1/10 scale articulated runner manikins were carried out. First, simple formations with one or two pacers were examined and the results were compared with previous investigations. Second, the runner formations of the Nike Breaking2 and INEOS 1:59 Challenge events whose goal was to break the 2 h marathon barrier were studied. The main finding was the identification of three complex formations of six and seven pacers that allow a drag-force reduction of about 60% with respect to a solo runner and an estimated time saving of 262 s. These results point to how it may be possible to run the fastest marathon ever.

1. Introduction

Elite male (female) marathoners are currently able to run the distance of 42.195 km at a speed of about 21 km h^{-1} (19 km h^{-1}). The last 50 years have seen significant improvements in the race performances. As an illustration, the progression in the race time of the

Electronic supplementary material is available online at https://doi.org/10.6084/m9.figshare.c.6761804.

THE ROYAL SOCIETY PUBLISHING

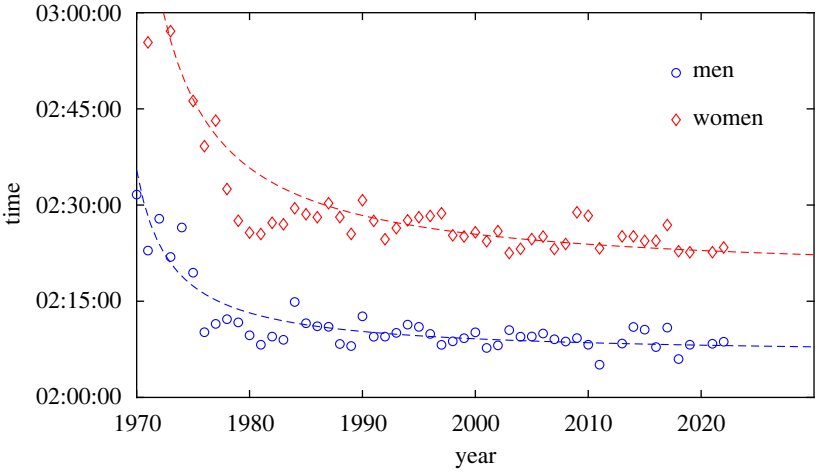

Figure 1. Evolution of the winning times at the New York City marathon [1].

New York City marathon is plotted in figure 1. Since the second victory of O. Pizzolato (2:11:34 in 1985) to the record for this race currently held by G. Mutai (2:05:05 in 2011), there has been a decrease of about 6 min over about 30 years. However, a plateau seems to have occurred for both men and women.

In recent years, the notion of marginal gains has been developed with the aim to further improve sport performances. The famous British cycling coach D. Brailsford summarized this concept in a well-known quotation [2], 'The whole principle came from the idea that if you broke down everything you could think of that goes into riding a bike, and then improved it by 1%, you will get a significant increase when you put them all together'. Although this idea was originally applied to cycling, it can be applied to many other sports, including running. Small enhancements via nutrition, altitude training, technical clothing, running shoes technology [3], continuous monitoring of physiological parameters [4,5], particular geometries of the athletic track [6], and even the influence of the facial expression [7] can together provide significant overall performance benefits.

In many sports, athletes race against the clock and aerodynamic drag is a determining factor. Drafting is a strategy whereby the air resistance acting on a designated athlete can be reduced by having other athletes positioned around him/her. This idea emerged very early in the scientific literature [8]. Drafting can be used in cycling [9–12], skating [13], and downhill skiing [14] among others. In marathon running, pacers can be positioned around a top runner to set the desired pace, but they also can decrease the drag force acting on a designated runner.

In 2017, as part of the Nike Breaking2 event in Monza, the now two-time Olympic marathon champion and world-record holder Eliud Kipchoge attempted to break the 2 h marathon barrier, recording a time of 2:00:25 [15]. This performance was made possible in part by a specific drag-reducing pacer formation with six runners forming an arrowhead in front of Kipchoge. A second attempt was made in 2019 as part of the INEOS 1:59 Challenge project in Vienna. Eliud Kipchoge broke the 2 h barrier with a time of 1:59:40.2. This result was achieved primarily via Kipchoge's incomparable running ability, but also through the consideration of many marginal gains, including a new formation of pacers as shown in figure 2. It is worth noting that both events involved a change-out of the pacers each lap. This characteristic violates the rules of World Athletics [17] and, therefore, the times were not recognized as true world records. However, a record-eligible cooperative drafting strategy was proposed [5].

Several numerical studies have investigated the effectiveness of different pacer formations in reducing the drag experienced by the central runner [4,18,19]. In addition, the benefit of running

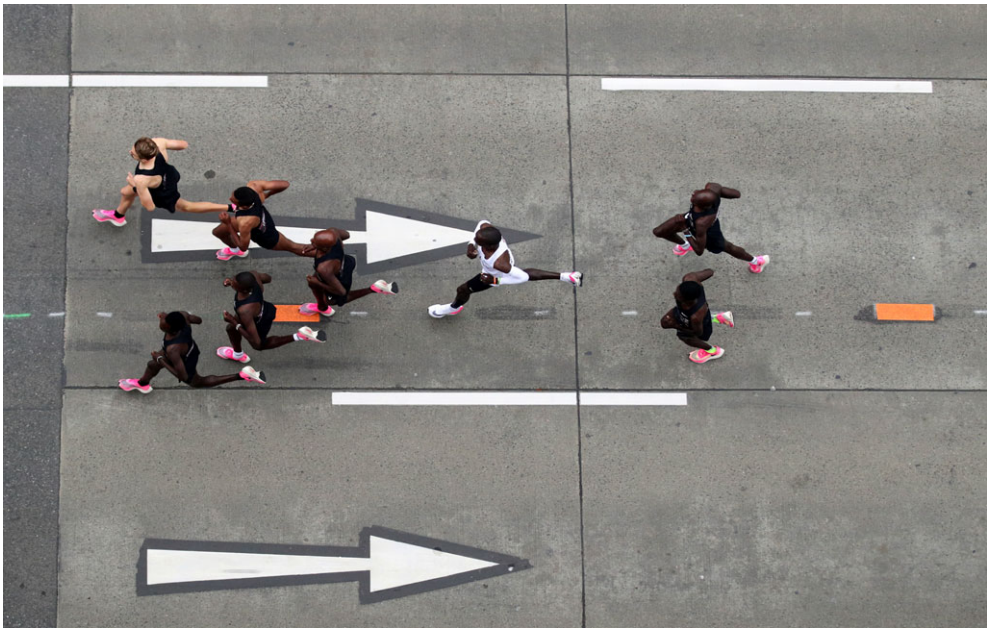

Figure 2. A moment of INEOS 1:59 Challenge in Vienna, Austria, (October 12, 2019) where Eliud Kipchoge was assisted by seven pacers, five forming an inverted arrow in front of him and two others behind him [16].

in formation by experimentally measuring the oxygen consumption of a solo runner, and also for a runner surrounded by other athletes, was evaluated in [4]. Experimental studies have also been conducted to characterize the aerodynamic drag of a runner. A treadmill system has been mounted in a wind tunnel in [20] to measure the drag on a solo runner modelled by an articulated manikin, and also with different duo running formations. The aerodynamic effects of clothing have also been investigated [21]. Finally, similar studies have estimated how the drag forces differ between peloton formations in cycling using experimental [12] and numerical approaches [22].

Pugh [23,24] and da Silva *et al.* [25] estimated the metabolic cost of a lone runner on a treadmill subjected to horizontal forces. In particular, a simple method that relates the reduction in drag force with drafting, to the reduction in gross metabolic power is introduced in the latter reference. These data are indeed used as input to evaluate the time saving [26] due to several pacer formations.

The aim of the present work was to experimentally investigate the aerodynamics of a group of runners in order to identify the pacer formations that allow the greatest time gains for a designated runner compared to a solo runner. Various formations of up to seven pacers were considered, including the configurations used in Nike Breaking2 and INEOS projects. To the knowledge of the authors, the drag force reductions afforded by these last two formations have not been published in peer-reviewed scientific journals [27–29]. The paper is organized as follows. The experimental set-up and the measurement techniques are introduced in §2. The results are reported in §3. Simple configurations are first discussed with the reference case of a solo runner examined in §3(a), and the case of a single and two pacers in §3(b). New complex formations with six or seven pacers are then in §3(c), one of which points to a possible significant time gain not only with respect to a solo runner configuration, but also in comparison with the two well-known formations mentioned above. Concluding remarks are finally provided in §4.

2. Experimental set-up and methodology

The measurements were performed in a wind tunnel of the Laboratoire de Mécanique des Fluides et d'Acoustique, a research facility already used in a recent sports aerodynamics study [12]. The

Figure 3. Marathoner manikin used in the present study: (*a*) front and side view; (*b*) manikin mounted in the wind tunnel.

Table 1. Values of the non-dimensional projected frontal area A/L^2 (RANS stands for Reynolds-averaged Navier–Stokes equations).

reference	A/L^2
present study (experiments)	0.144
Hill [30] (experiments)	0.146
Pugh [24] (experiments)	0.147
Davies [31] (experiments)	0.136–0.152
Kipp *et al*. [26] (experiments)	0.154
Beaumont *et al*. [4] (RANS)	0.165
Polidori *et al*. [18] (RANS)	0.174
Schickhofer & Hanson [19] (RANS)	0.161

wind tunnel is 1.5 m long with a 40×40 cm square cross-section. Identical articulated manikin runners at scale 1/10 of $L = 17$ cm high are shown in figure 3. The projected frontal area estimated from a computer-aided design software is $A = 0.00416\,\mathrm{m}^2$, leading to a ratio between the frontal section and the height squared of the manikin of $A/L^2 = 0.144$. This value is consistent with those found in previous studies, summarized in table 1.

A suitable aluminium perforated plate comprised the floor of the wind tunnel. The plate was designed to fix each pacer as desired around the designated runner and comprises a square grid of $\Delta = 15$ mm allowing us to explore various pacer formations. The designated runner positioned in the middle of this grid was attached on a circular support in poly(methyl methacrylate) of 86 mm diameter which was directly linked to a load cell which measured two force components, namely in the flow direction and normal to the flow direction. The grid holes not used during the measurements were covered with metallic duct tape in order to not disturb the flow.

The measurements were carried out at ambient atmospheric pressure and temperature of about 20°C, corresponding to an air density $\rho \simeq 1.20\,\mathrm{kg\,m^{-3}}$. The free stream velocity U was obtained from a Pitot tube with an accuracy of $\pm 0.1\,\mathrm{m\,s^{-1}}$. The turbulent flow was also characterized in a previous investigation [12] by means of a single hot-wire anemometer. The

thickness of the boundary layer developing at ground level was found to be less than 0.4 cm. This value is significantly below the ankles of the manikin runner and it should not impact the accuracy of the forces measured by the aerodynamic balance [22]. The measured value of the free-stream turbulent intensity was approximately 0.5%.

The Reynolds number was calculated from the height of the manikin [19] as follows:

$$Re = \frac{UL}{\nu}, \tag{2.1}$$

where $\nu \simeq 1.51 \times 10^{-5}\,\mathrm{m\,s^{-2}}$ is the kinematic viscosity of air at 20°C. For a full-scale marathoner running at 21 km h^{-1} $\simeq 5.8\,\mathrm{m\,s^{-1}}$ and a height of $L = 1.7$ m, the associated Reynolds number value is $Re \simeq 6.6 \times 10^5$. In the experiments, for a $L = 17$ cm high manikin and a flow speed $U = 25\,\mathrm{m\,s^{-1}}$, $Re \simeq 2.8 \times 10^5$, a value lower by a factor of about two. The aerodynamic drag force F_D experienced by the designated runner model was measured with a load cell with a resolution of 0.01 N. The data were sampled at 10 Hz for 10 s and an averaged value was recorded. The force measurements were repeated between 30 to 50 times, and the experimental uncertainty [32] was estimated as approximately ±3% in the velocity range $U = 10 - 25\,\mathrm{m\,s^{-1}}$. The force F_D is related to the drag coefficient C_D by the following relationship:

$$F_D = \frac{1}{2}\,\rho\, U^2 A\, C_D, \tag{2.2}$$

where the drag coefficient is expected to be a function of the Reynolds number only, $C_D = C_D(Re)$, to justify the similitude analysis.

In the present experimental study, we adopted some simplifications that could affect the results. The manikin runner has its own body proportions which do not exactly match those of a real runner, even if the estimate of projected frontal area is quite consistent with the values of previous studies. The manikins were fixed in the wind tunnel frame and air was moving, which is the opposite during a real race. A boundary layer develops along the floor, but, as noted earlier, its thickness has been found to be small in the present experimental set-up. The manikin runners maintain a static position during the experiments and the effects induced by the motion of the body and limbs (arms and legs) are therefore neglected. Only discrete positions are possible between two runners but the grid step size Δ provided by the distance between two holes was small. It can be compared to the practical distance of about 1.3 m between two runners using cooperative drafting [18,19] for instance.

Finally, the Reynolds number was approximately two times lower in the experiments compared to full-scale human runners. For this range of Reynolds number values, the drag crisis has already occurred and the drag coefficient reaches a plateau and is insensitive to changes in Re, remaining of the same order of magnitude as discussed in the next section. This difficulty is also encountered in numerical simulation when a turbulence model is used to solve the Reynolds-averaged Navier–Stokes equations, refer to table 1. Numerical predictions are almost independent of the Reynolds number value [33], and specific formulations must be used for the prediction of boundary layer transition for instance.

3. Results

The experiments focused on three main aspects of the running aerodynamics. Firstly, we considered the aerodynamics of a solo runner in order to compare and validate our measurements against available data. Then, simple formations with one or two pacers were studied to estimate the drag reduction with respect to the solo runner case. The most advantageous drafting formations have been identified as when the designated runner is positioned in the wake of the pacers. Finally, more complex formations of six or seven pacers have been investigated and the advantages of drafting in terms of race-time saving by applying a simplified model have been estimated [25,26].

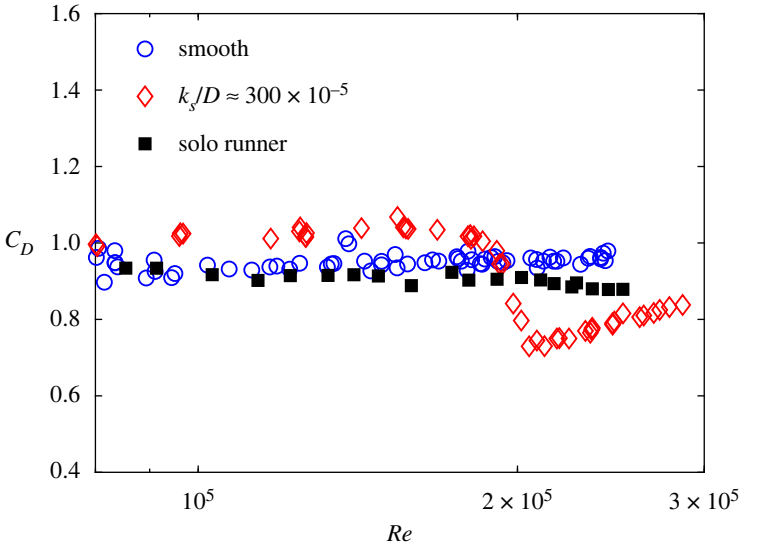

Figure 4. Measured drag coefficient C_D as a function of Re for a finite-length circular cylinder with an aspect ratio $L/D \simeq 2.9$: smooth cylinder (circle), rough cylinder (diamond); and for the solo runner manikin (square).

(a) Solo runner

The study of a solo runner was an essential first step of the present analysis. The average solo drag coefficient was used as a reference value, to be compared to the coefficients obtained for the various pacer formations. The experimental protocol was also validated, by first comparing a smooth and a rough finite-length cylinder. The drag force has also been measured for different postures of a solo runner to evaluate the sensitivity of C_D with respect to these changes in limb positions.

(i) Finite-length cylinder

The drag coefficient of both smooth and rough finite-length cylinders of dimensions close to those of the runner manikin were first measured. Both cylinders have a height of $L = 17.5$ cm and a diameter of $D = 6$ cm, which provide an aspect ratio $L/D \simeq 2.9$. The roughness coefficient has been estimated to be about $k_s/D \simeq 300 \times 10^{-5}$ for the second cylinder, where k_s is the equivalent sand-grain roughness [34]. Note that the Reynolds number is still based on L to be consistent with equation (2.1), and not the diameter as done usually [34,35]. The experimental results are plotted in figure 4, where C_D is calculated by taking for the frontal area $A = D \times L$. A plateau can be observed for the measured drag acting on the smooth cylinder with $C_D \simeq 0.95$. The empirical relation derived by Uematsu & Yamada [35,36] in the subcritical flow regime,

$$C_D \simeq 1.2 \left\{ 0.58 + 0.17 \left[\ln\left(\frac{L}{D}\right) \right]^{1.6} \right\}, \tag{3.1}$$

provides the value $C_D = 0.92$, close to the measured value. The flow velocity limit of the wind tunnel did not allow transition of the boundary layer on the cylinder surface.

Conversely, a drag crisis with an abrupt decrease to about 0.3 of C_D occurs for the rough cylinder at $Re \simeq 1.9 \times 10^5$, in agreement with previous studies in similar conditions, namely $L/D = 3$ and $k_s/D \simeq 500 \times 10^{-5}$ in [35]. Transition of the boundary layer is sensitive to the surface roughness, and occurs at a lower Reynolds number value with respect to the smooth case. Furthermore, the drag coefficient takes higher values before and after the drag crisis. One gets

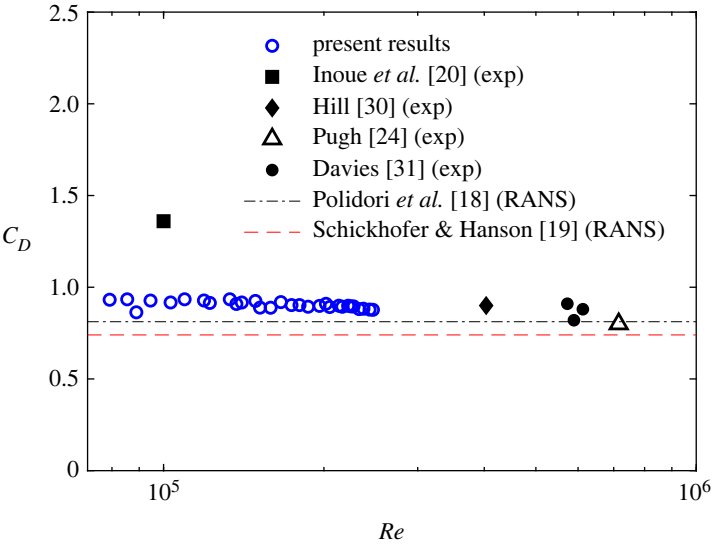

Figure 5. Drag coefficient: present results (circle), data found in various experimental [20,24,30,31] and numerical [18,19] studies for a solo runner as a function of the Reynolds number.

for instance $C_D \simeq 1.03$ in the subcritical flow regime for the rough finite-length cylinder. This academic case of the finite-length cylinder illustrates the good quality of the facility.

(ii) Solo runner model

The runner manikin shown in figure 3 can be considered as a bluff body with sharp edges and a large frontal area, which induce a strong flow separation. The drag force is dominated by the pressure contribution and the dependence on the Reynolds number is expected to be negligible. The measured drag coefficient is superimposed in figure 4, and is found to be reasonably constant between $Re \simeq 8 \times 10^4$ and 2.8×10^5, corresponding to a wind tunnel velocity range of $U \simeq 10$–$25\,\mathrm{m\,s^{-1}}$. The measured values are compared to values found in other experimental [20,24,30,31] and numerical [18,19] studies in figure 5. A reasonable agreement is observed. The dispersion may be related to the different models used, or to the turbulence model for numerical predictions which systematically underestimates experimental values. This analysis shows that our set-up with a slightly lower Reynolds number allows us to study several aspects of running aerodynamics in a manner consistent with what would be obtained for a full-scale runner. The present values of the drag coefficient are also in agreement with the pioneering work by Hill [30]. The velocity values used to estimate the drag coefficient are however not provided in the Hill study. For the computation of the Reynolds number, the height of the runner model (8 inches), the air kinematic viscosity at 15°C, and the maximum achievable velocity value of about $30\,\mathrm{m\,s^{-1}}$ in the wind tunnel of the National Physical Laboratory [37] have been used.

(iii) Changes in posture

The influence of a variation in runner posture on the drag force was examined for two cases with respect to the reference case of a runner-like position during the stride, namely a posture with outstretched arms and a position with one leg wide apart, as shown in figure 6. A relative variation of just 0.55% is found in the former case, and of 2.53% in the last case for the drag coefficient. These results show that even large and quite unnatural variations in posture have only slight effects on the values of C_D and they remain lower than 3% with respect to the more realistic position. In what follows, all the runner manikins were mounted in the wind tunnel in the reference running position (figures 3*a* and 6*a*).

Figure 6. Changes in marathoner's position: reference running position (*a*), outstretched arms (*b*) and one leg wide apart (*c*).

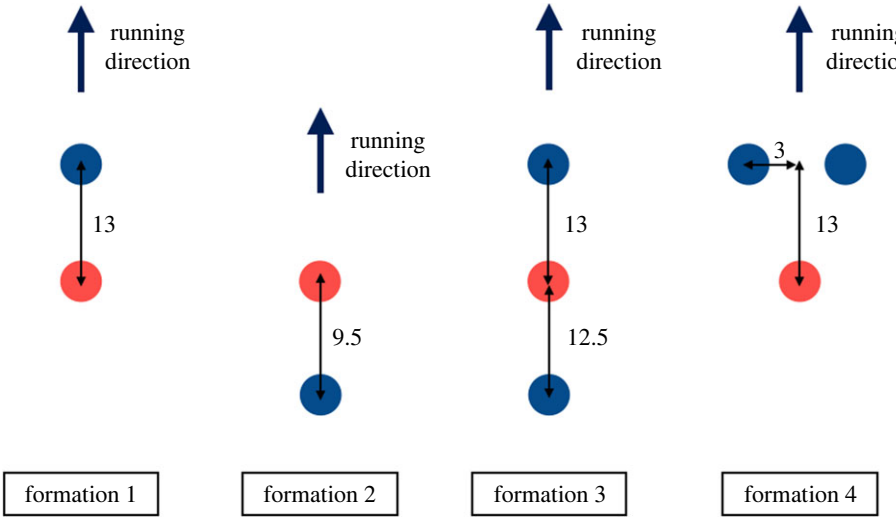

Figure 7. Top view of pacer formations in scaled wind tunnel testing (distances in centimetres). The designated runner is indicated by the red circle, and the pacers are indicated by the blue circles.

(b) Simple formations with one or two pacers

(i) Drag coefficient of simple formations

Simple formations involving one and two pacers were examined, by considering the drag-force reduction observed on the designated runner (in red) as shown in figure 7. For each of the four configurations, a series of measurements at the maximum wind tunnel velocity $U \simeq 25\,\mathrm{m\,s^{-1}}$ was carried out. The relative changes

$$\Delta C_D = \frac{C_D - C_D^\star}{C_D^\star}, \tag{3.2}$$

Table 2. Relative variation ΔC_D for simple formations (refer to figure 7) with respect to a solo runner.

formation	#1	#2	#3	#4
present study (experiments)	−39.5%	−4.0%	−42.7%	−37.0%
Schickhofer & Hanson [19] (RANS)	−70.1%	—	−75.6%	−41.3%
Beaumont *et al.* [4] (RANS)	—	—	−33%	—
Polidori *et al.* [18] (RANS)	−55.3%	—	—	−38.5%

of the designated runner drag coefficient with respect to a solo runner were then calculated, and compared with some previous numerical studies [4,18,19]. The results are gathered in table 2. The reference drag coefficient was taken to be equal to $C_D^\star = 0.88$, the value measured in the previous section for the highest wind tunnel velocity, see figure 5.

A spectacular air-resistance reduction $\Delta C_D \simeq 40\%$ is observed when a single pacer is placed before the designated runner, the formation 1 in figure 7. The experiments were performed at a 1/10 scale for lengths, which means that the real distance between the two runners equates to 1.3 m at full scale, a realistic value as already mentioned previously. By convention, the distance between runners was measured as the distance between the tips of their left feet. One runner placed behind the designated runner (formation 2) provides a smaller but not negligible improvement. That is relevant for the cooperative drafting concept [5]. Formation 3 is a combination of the formations 1 and 2 and confirms that the rear pacer provides a contribution that can not be neglected. Formation 4 with two pacers placed equidistant in front of the designated runner does not show any further benefit since the drag-force reduction is somewhat less than in formation 1.

The comparison with the numerical studies of Beaumont *et al.* [4] and Polidori *et al.* [18] shows a fairly good agreement, as reported in table 2. Note that in the Polidori *et al.* [18] study, slightly different formations where three pacers were positioned in front of the designated runner were analysed. Conversely, some large discrepancies are identified with the numerical solutions of Schickhofer & Hanson [19], for both formations 1 and 3, whereas a better agreement is found for formation 4.

(ii) Influence of the distance between runners on the drag coefficient

A parametric study was conducted regarding the influence of the distance d between the two runners on the drag coefficient in formations 1 and 2 shown in figure 7. Three cases were investigated as shown in figure 8: the variation of the longitudinal distance of the front (case 1) and back pacer (case 2), and the variation of the lateral position of the front pacer (case 3).

The variation of C_D with respect to the distance d between the designated runner and a front pacer (case 1), normalized by the runner height L, is plotted in figure 9. The drag coefficient exhibits a nonlinear rise as d/L increases and reaches a plateau for $d > 2L$. The slipstreaming is still somewhat effective with the air-resistance reduction being about 20%. This result demonstrates the extreme importance of the front pacer and the effectiveness of the formation 1. As already shown by other authors [19,20], the gain significantly increases as the pacer gets closer than $d = L$. It is therefore crucial to know what is the minimum distance that can be maintained between the designated runner and the pacers in order to maximally reduce the air resistance without disturbing the designated runner. The answer to this problem cannot be fully analysed with runner manikins since parameters such as the stride length and also psychological factors must be taken into account. As an illustration, the value of the INEOS 1:59 Challenge formation analysis was set at 1.75 m, but Schickhofer *et al.* [19] used a distance of 1.3 m and Pugh [24] assumed a value of 1.0 m.

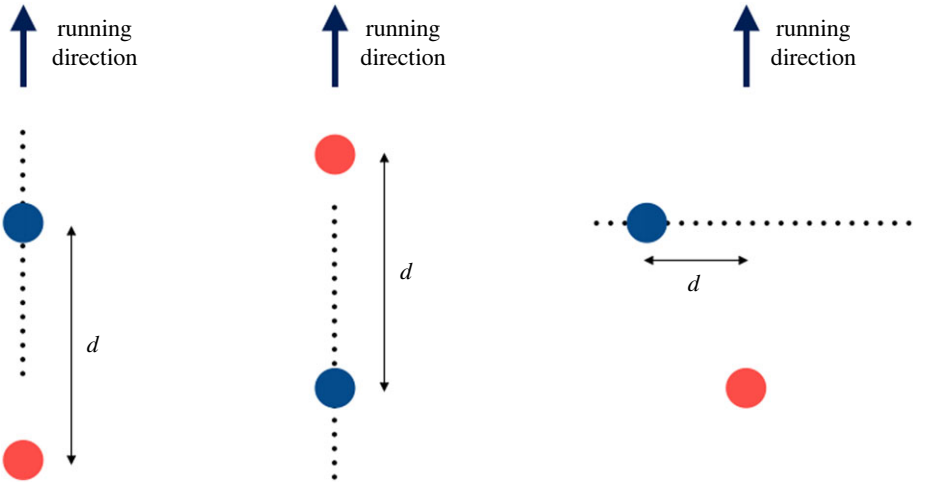

Figure 8. Top view of pacer formations in scaled wind tunnel testing. The designated runner is indicated by the red circle and the pacers are indicated by the blue circles. The quantity d represents the longitudinal (or lateral) distance between the designated runner and the pacer.

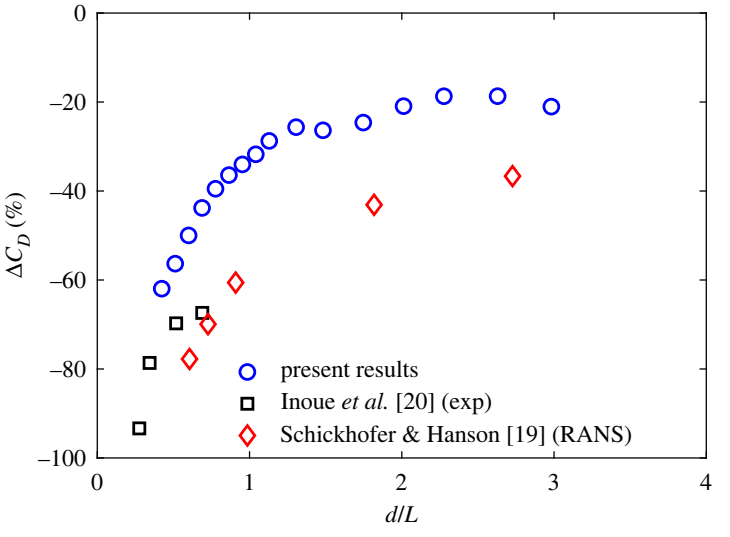

Figure 9. Relative variation of C_D for the designated runner as a function of the longitudinal non-dimensional distance d/L between one leading pacer and the designated runner (see figure 8, case 1).

A similar study was performed to examine the influence of a rear pacer at varying distances from the designated runner (case 2), and results are plotted in figure 10. Three distinct zones can be identified. In the range $0.5L < d < 0.9L$, the drag coefficient remains constant with an average relative variation $\Delta C_D \simeq 4.3\%$. As shown in the numerical simulations [19], a runner produces a wake region of about 0.7 L characterized by a negative pressure coefficient and also a smaller frontal region with a positive pressure coefficient. A designated runner located within this frontal region thus benefits from a propulsive force from behind that contributes to the reduction of C_D. As the rear pacer moves further back, the designated runner leaves this region and the drag coefficient starts to rise until $d \simeq 1.5$ L where it reaches a new plateau with $\Delta C_D \simeq 1.7\%$. This result

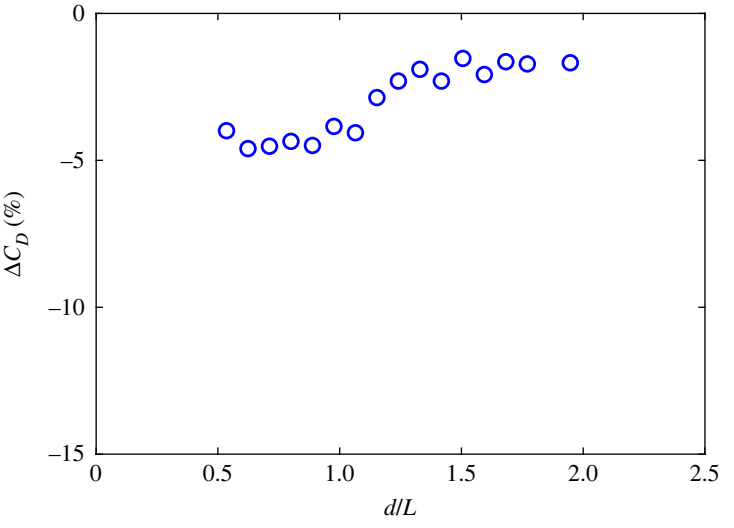

Figure 10. Relative variation of C_D with respect to a solo runner as a function of the normalized rear pacer position d/L (see figure 8, case 2).

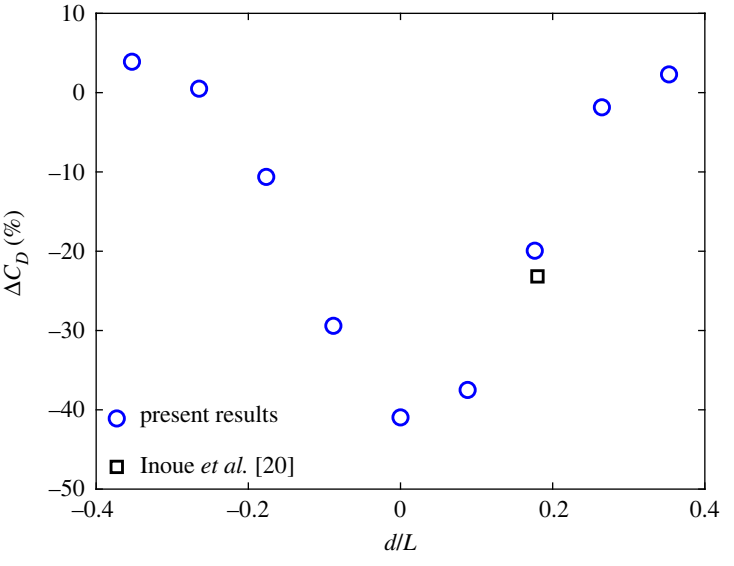

Figure 11. Relative variation of C_D with respect to a solo runner as a function of the normalized lateral position d/L of the leading runner (see figure 8, case 3).

shows the positive effect of placing of one pacer (or more) behind the designated runner in the range 1.0–1.5 m at full scale.

The change in drag coefficient when the lateral distance between the runner and the pacer varies (case 3) has also been investigated, and results are plotted in figure 11. A symmetric curve centred on $d = 0.07$ L is obtained, noting that the position of the pacer is located on his left foot, refer to figure 8. The effectiveness of drafting decreases as the leading runner increases the lateral distance. Combined with the results of figure 9, this analysis shows that, as expected, the maximum reduction of C_D is reached when the front pacer is located in the central position and as near as possible to the designated runner. The point studied by Inoue *et al.* [20] is also

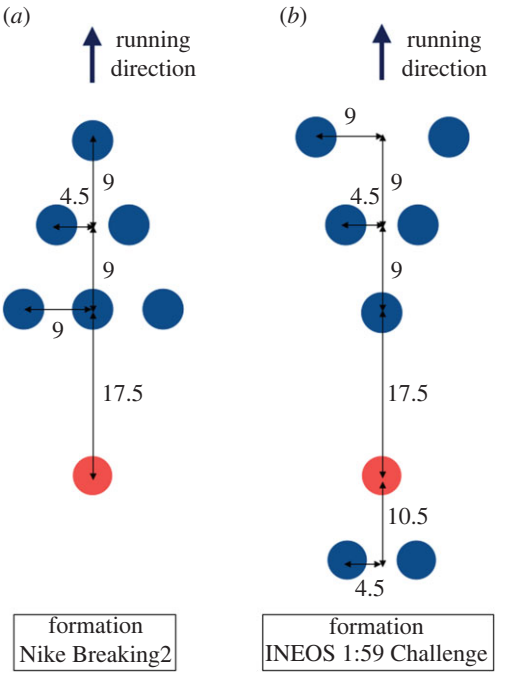

Figure 12. Top view of pacer formations in scaled wind tunnel testing (distances in centimetres). The designated runner is indicated by the red circle and the pacers are indicated by the blue circles. Formations adopted during Nike Breaking2 (*a*) and INEOS 1:59 Challenge (*b*).

superimposed in figure 11, in agreement with the present data. The longitudinal distance between the front pacer and the designated runner is slightly different; 0.69 L in [20] and 0.78 L in the current study.

(c) Complex formations of pacers

Finally, we investigated some complex and novel formations involving six and seven pacers in order to identify the most effective formation in terms of drag-force reduction on the designated runner. We replicated the pacer formations of the Nike Breaking2 and INEOS 1:59 Challenge events in wind tunnel experiments. In Nike Breaking2, six pacers formed an arrowhead in front of the designated runner as displayed in figure 12*a*. In the INEOS 1:59 Challenge, five pacers formed an inverted arrowhead in front of the designated runner and two other pacers were in the back, see figures 12*b* and 13. The drag reductions with respect to a solo runner, measured for these two configurations, are reported in table 3. The pacer configuration of Nike Breaking2 allows a drag-force reduction of 39.7%, whereas in the INEOS 1:59 Challenge ΔC_D reaches 50.2%. The greater efficiency of the INEOS formation is perhaps not surprising since Eliud Kipchoge used it when he broke the 2 h marathon barrier in 2019.

Several other formations of six or seven pacers were also evaluated in order to explore if there is a formation that further reduces drag compared to the formation of the INEOS 1:59 Challenge. The positions of the pacers are shown in figure 14. Two of these configurations, namely numbers 5 and 7, were more effective than the INEOS 1:59 Challenge whereas the formation 6 was less effective, as reported in table 3. A decrease in the drag force similar to that of INEOS 1:59 Challenge is obtained with the formation 7 by using only six pacers, not seven. This is another relevant marginal gain when one has to conceive race strategies.

The promising results obtained with the formation 7 motivated the final experiment (formation 8, referred to as swordfish-like configuration) and with three variants of this configuration, as

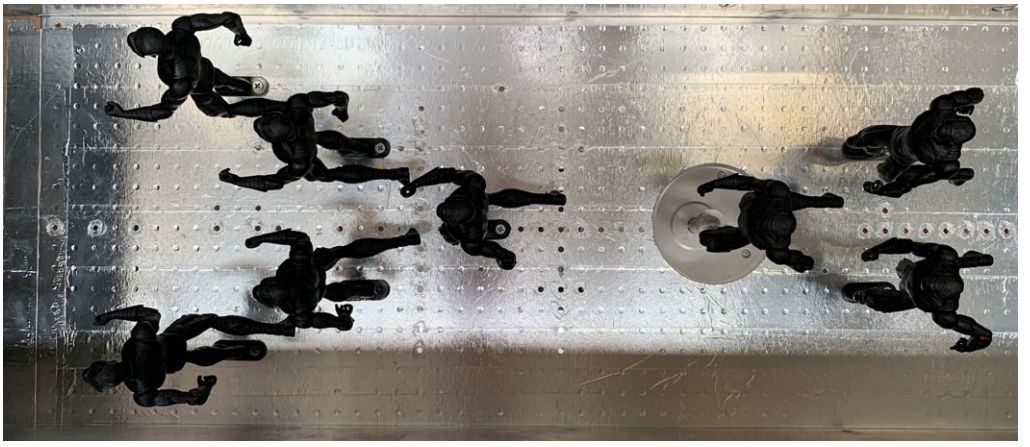

Figure 13. Wind tunnel experiments of the pacer formation used in the INEOS 1:59 Challenge.

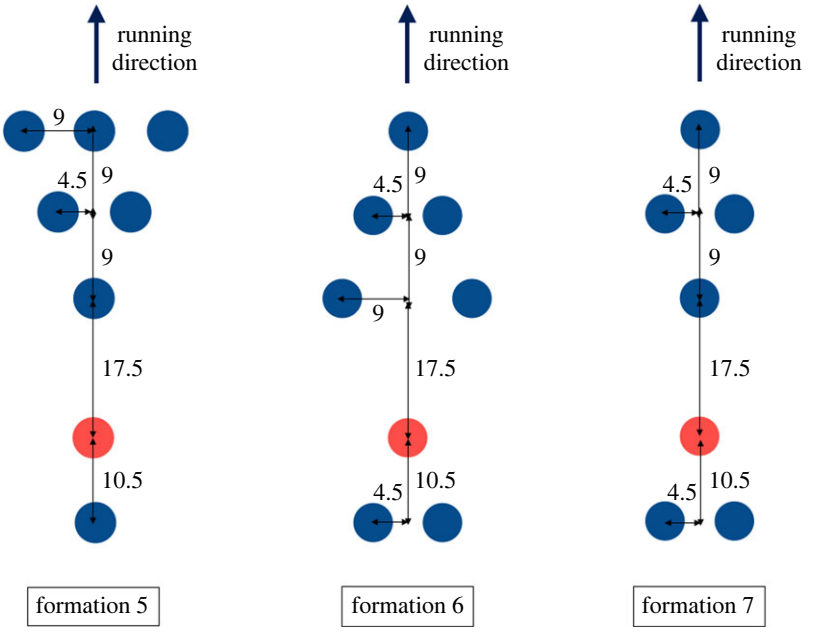

Figure 14. Top view of pacer formations in scaled wind tunnel testing (distances in centimetres). The designated runner is indicated by the red circle and the pacers are indicated by the blue circles. Novel complex pacer formations.

shown in figure 15. An additional pacer was included, and a variation of the distance between the designated runner and the front pacer was considered. The three configurations provide similar results, and remarkably offer a further 10% reduction in drag beyond the INEOS 1:59 Challenge formation (table 3). Such results show the importance of the front pacers in reducing C_D and open up interesting perspectives for future marathon record attempts.

An estimate of the time saving associated with the complex configurations examined in this section was finally computed. To do this, we applied the relationship proposed by da Silva *et al.* [25]. They found that the average change in gross metabolic power ΔP_{meta} was 6.13% per 1% body weight of horizontal impeding force, here represented by the aerodynamic drag. Running

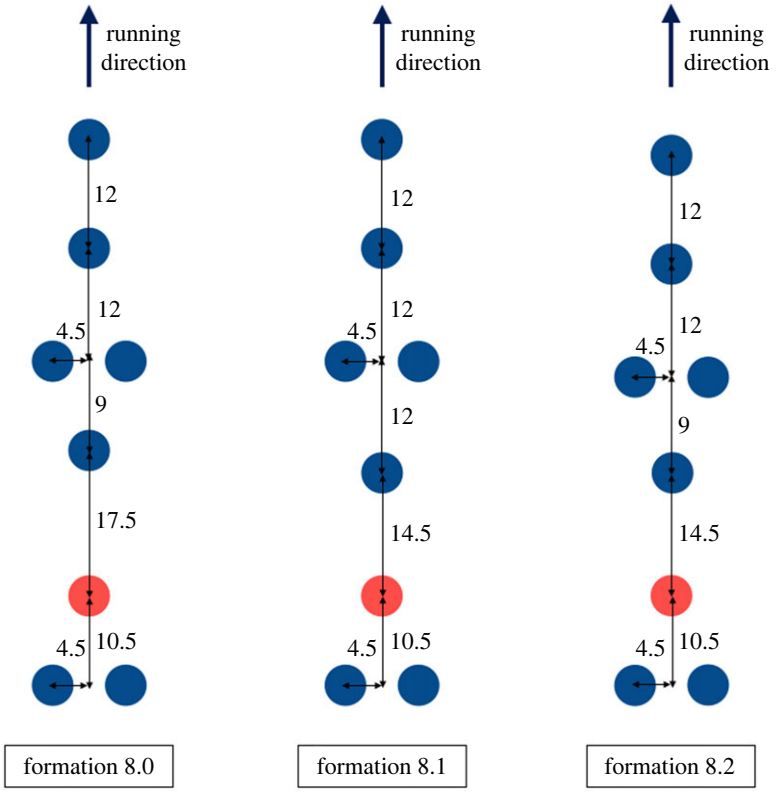

Figure 15. Top view of pacer formations (swordfish-like configuration) in scaled wind tunnel testing (distances in centimetres). The designated runner is indicated by the red circle and the pacers are indicated by the blue circles. Variants of the previous formation 7 (figure 14) with an additional pacer.

Table 3. Relative drag reduction ΔC_D, see equation (3.2), and estimates of the time savings with respect to a solo marathon runner using the models of [25,26].

formation	ΔC_D	time saving (mm:ss)
Nike Breaking2	−39.7%	2:49
INEOS 1:59 Challenge	−50.2%	3:33
formation 5	−53.0%	3:45
formation 6	−30.8%	2:12
formation 7	−51.5%	3:38
formation 8.0	−60.3%	4:15
formation 8.1	−62.1%	4:22
formation 8.2	−61.0%	4:17

economy (RE) is a key quantity in sports physiology and corresponds to the rate of oxygen uptake for running at a specified velocity.

The time savings in the different configurations were calculated with respect to the race time $t^\star$ performed by Eliud Kipchoge during the Berlin marathon in 2018, during which he set the world record 2:01:39. The reference velocity was $U^\star \simeq 5.78\,\mathrm{m\,s^{-1}}$, associated with the drag force of a full-scale solo runner, $F_D^\star = 7.50$ N. The new velocity U associated with the aerodynamic drag force

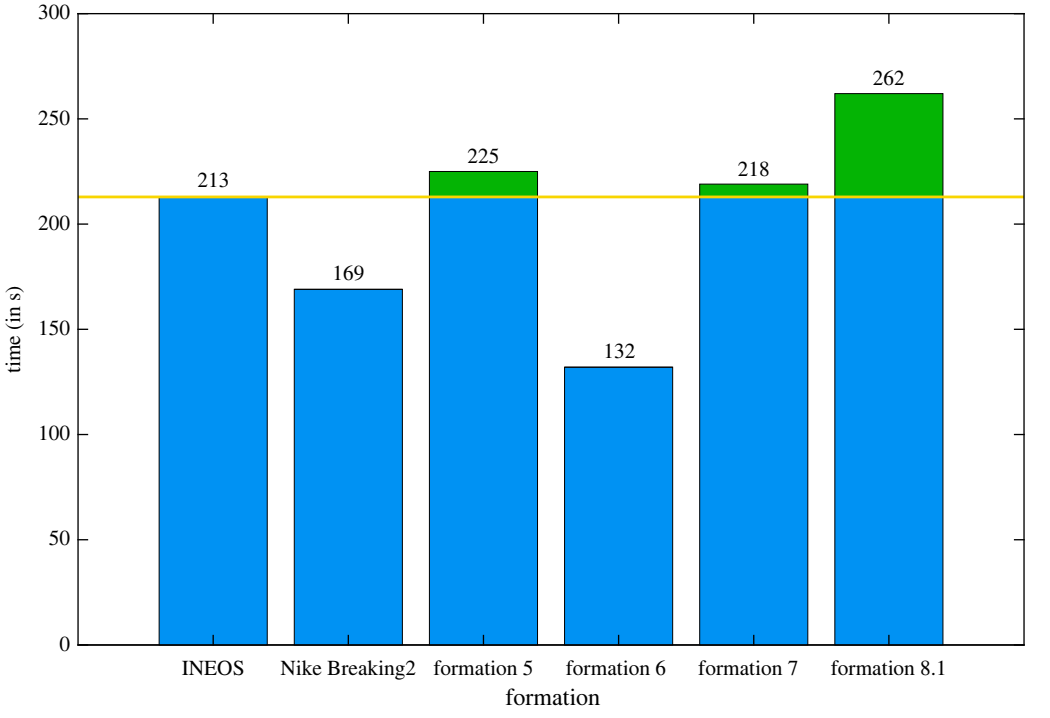

Figure 16. Time savings for different formations with respect to a solo runner computed with the models of [25,26].

F_D (and, therefore, with the drag coefficient C_D) of the drafting formation was then estimated by linearizing the relation between RE and U around the reference point $U^\star$ here [26]

$$U = U^\star(1 + \alpha\, \Delta RE), \tag{3.3}$$

where the coefficient $\alpha \simeq 2/3$ for the typical velocity $U^\star$ of an elite marathoner. The variation of the running economy was assumed as $\Delta RE \simeq \Delta P_{\text{meta}}$, where we used the body mass of Kipchoge ($m_r = 52$ kg) to estimate the reduction in the gross metabolic power [25]

$$\Delta P_{\text{meta}} \simeq 0.0613\, \Delta C_D\, \frac{F_D^\star}{m_r\, g}, \tag{3.4}$$

with g the acceleration of gravity. The race times over the distance of a marathon were estimated for the formations described in figures 12, 14 and 15, and the time savings were reported in table 3. The results were also plotted more explicitly in figure 16.

The predicted time for the INEOS 1:59 Challenge is equal to 1:57:39, approximately 2 min lower than the real time 1:59:40. A significant discrepancy is also found for the Nike Breaking2 event where the prediction is 1:58:23 and the actual time was 2:00:25. As suggested in [25,38] the drafting can reduce convective cooling and that implies unfavourable conditions in hot or humid ambient. The time saving observed for formation 8.1 is quite significant even if that estimate could be affected from some uncertainties.

4. Conclusion

Wind tunnel experiments at 1/10 scale with static, articulated manikins were performed to measure the aerodynamic drag reductions provided to a designated runner by various drafting formations. With the aim to break race records on a marathon distance, an elite runner of height $L = 1.7$ m and velocity $U = 21$ km h^{-1} was considered, leading to a Reynolds number value $Re \simeq 6.6 \times 10^5$ at full scale.

The experimental process was first validated by considering a smooth and rough finite-length cylinder, and then a solo runner. The drag crisis was clearly identified for the former case whereas the drag coefficient of the solo runner was found to be nearly constant. A large flow separation was indeed expected for the runner manikin, in agreement with bluff body aerodynamics. The small reduction in the Reynolds number value for the similitude $Re \simeq 2.8 \times 10^5$ in experiments is thus not expected to have any influence with what would be obtained for a full-scale runner. The value found for the drag coefficient is also in agreement with previous studies. Simple formations of pacers were then investigated, and the measured drag reductions were in good agreement with previous studies. In particular, the importance of positioning pacers in close proximity to the designated runner was quantified. Complex formations of six and seven pacers including the Nike Breaking2 and INEOS 1:59 Challenge formations were examined in the second part of the present study, and the time savings were estimated using the best physiological relationships representing the current state of knowledge. A reasonable agreement is found for the INEOS 1:59 Challenge formation, and more of interest, three new configurations in swordfish-like profile have been identified to be more effective in terms of drag reduction, with an additional enhancement of about 10%. To the knowledge of the authors, these experimental results have never been provided in the scientific literature previously. These findings could be of interest in defining new team strategies to break records by following a marginal gain approach. Our findings could be refined using numerical simulations that elucidate the specific factors that lead to the drag reductions for the designated runner.

Data accessibility. The data are provided in electronic supplementary material [39].

Declaration of AI use. We have not used AI-assisted technologies in creating this article.

Authors' contributions. M.M.: conceptualization, data curation, formal analysis, investigation, methodology, project administration, resources, supervision, validation, visualization, writing—original draft, writing—review and editing; J.L.: conceptualization, investigation, writing—original draft, writing—review and editing; E.R.: conceptualization, investigation, writing—original draft, writing—review and editing; P.S.: conceptualization, formal analysis, funding acquisition, investigation, methodology, project administration, supervision, validation, visualization, writing—original draft, writing—review and editing; C.B.: conceptualization, formal analysis, funding acquisition, investigation, methodology, project administration, supervision, validation, visualization, writing—original draft, writing—review and editing.

All authors gave final approval for publication and agreed to be held accountable for the work performed therein.

Conflict of interest declaration. We declare we have no competing interests.

Funding. No funding has been received for this article.

Acknowledgements. The authors would like to express their gratitude to Horacio Correia for the realization of the experimental set-up and for his valuable technical support for the wind tunnel measurements. The authors are grateful to an anonymous referee for helpful comments.

Appendix A. Full-scale drag force

The numerical value of the drag force F_D experienced by a full-scale designated runner is collected in table 4 from various studies, and by assuming for the running velocity $U = 21\,\mathrm{km\,h^{-1}}$, for the frontal area $A = 0.419\,\mathrm{m^2}$ [25], and by taking dry air 15°C at sea level, $\rho = 1.225\,\mathrm{kg\,m^{-3}}$.

It is worth noting that the pacer formations evaluated in [27,29] slightly differ from the configurations, respectively, adopted in the Nike Breaking2 and the INEOS 1:59 Challenge events, as shown in figure 12. Beves & Ferguson [27] numerically simulated a formation with an additional pacer behind the designated runner. Blocken [29] performed wind tunnel experiments and numerical simulations for a ten pacer formation, seven placed in front and three behind the designated runner. These differences could partially explain the large discrepancies in the drag-force values observed in table 4.

Table 4. Full-scale values of the drag force F_D (N) experienced by the designated runner for different pacer formations.

formation	reference	drag force F_D (N)
solo runner	present study	7.68
	Hill [30]	7.86
	Pugh [24]	6.99
	Davies [31]	7.60
	Inoue *et al.* [20]	11.88
	Polidori *et al.* [18]	7.09
	Schickhofer & Hanson [19]	6.46
	da Silva *et al.* [25]	7.01
formation #1	present study	4.65
	Polidori *et al.* [18]	3.17
	Schickhofer & Hanson [19]	1.93
formation #3	present study	4.40
	Schickhofer & Hanson [19]	1.58
formation #4	present study	4.84
	Schickhofer & Hanson [19]	3.79
	Polidori *et al.* [18]	4.36
Nike Breaking2	present study	4.63
	Beves & Ferguson [27] (see comment)	1.95
INEOS 1:59 challenge	present study	3.82
	Blocken [29] (see comment)	1.05
formation #7	present study	3.72
formation #8.1 (swordfish)	present study	2.91

References

1. The Editors of Encyclopaedia Britannica. 2022 New York City Marathon. See www.britannica.com/sports/New-York-City-Marathon.
2. BBC Sport MS. 2012 Olympics cycling: Marginal gains underpin Team GB dominance. See www.bbc.com/sport/olympics/19174302.
3. Hoogkamer W, Kipp S, Frank JH, Farina EM, Luo G, Kram R. 2018 A comparison of the energetic cost of running in marathon racing shoes. *Sports Med.* **48**, 1009–1019. (doi:10.1152/japplphysiol.00086.2022)
4. Beaumont F, Bogard F, Murer S, Polidori G, Madaci F, Taiar R. 2019 How does aerodynamics influence physiological responses in middle-distance running drafting? *Math. Model. Eng. Probl.* **6**, 129–135. (doi:10.18280/mmep.060117)
5. Hoogkamer W, Snyder K, Arellano C. 2018 Modeling the benefits of cooperative drafting: is there an optimal strategy to facilitate a sub-2-hour marathon performance? *Sports Med.* **48**, 2859–2867. (doi:10.1007/s40279-018-0991-4)
6. Aftalion A, Trélat E. 2020 How to build a new athletic track to break records. *R. Soc. Open Sci.* **7**, 200007 (doi:10.1098/rsos.200007)
7. Brick NE, McElhinney MJ, Metcalfe RS. 2018 The effects of facial expression and relaxation cues on movement economy, physiological, and perceptual responses during running. *Psychol. Sport Exerc.* **34**, 20–28. (doi:10.1016/j.psychsport.2017.09.009)
8. Kyle CR. 1979 Reduction of wind resistance and power output of racing cyclists and runners travelling in groups. *Ergonomics* **22**, 387–397. (doi:10.1080/00140137908924623)

9. Malizia F, Blocken B. 2020 Bicycle aerodynamics: history, state-of-the-art and future perspectives. *J. Wind Eng. Ind. Aerod.* **200**, 104134 (doi:10.1016/j.jweia.2020.104134)
10. Malizia F, Blocken B. 2021 Cyclist aerodynamics through time: better, faster, stronger. *J. Wind Eng. Ind. Aerod.* **214**, 104673 (doi:10.1016/j.jweia.2021.104673)
11. Clanet C, Abel H, Brunet E, Grasso F, Robert C, Cohen C. 2021 Cycling speeds in crosswinds. *Phys. Rev. Fluids* **6**, 124601 (doi:10.1103/PhysRevFluids.6.124601)
12. Kraemer P, Marro M, Correia H, Salizzoni P. 2021 Preliminary study on crosswind aerodynamics for a group of road race cyclists. *SN Appl. Sci.* **3**, 279 (doi:10.1007/s42452-021-04233-z)
13. D'Auteuil A, Larose G, Zan S. 2012 Wind turbulence in speed skating: measurement, simulation and its effect on aerodynamic drag. *J. Wind Eng. Ind. Aerod.* **104–106**, 585–593. (doi:10.1016/j.jweia.2012.02.002ISTEX)
14. Brownlie L. 2021 Aerodynamic drag reduction in winter sports: the quest for 'free speed'. *Proc. Inst. Mech. Eng. P: J. Sports Eng. Technol.* **235**, 365–404. (doi:10.1177/1754337120921091)
15. Mulkeen J. 2017 Kipchoge a 'happy man' in Monza (Online). See www.worldathletics.org/news/report/breaking-2-marathon-eliud-kipchoge-monza (accessed 26 July 2022).
16. ineos.com. 2019 1:59:40.2: the INEOS 1:59 performance blueprint (Online). See www.ineos159challenge.com/ (accessed 19 July 2022). Image by REUTERS/Lisi Niesner
17. IAAF. 2017 *Competition rules 2018–2019*. International Association of Athletics Federations, Monaco.
18. Polidori G, Legrand F, Bogard F, Madaci F, Beaumont F. 2020 Numerical investigation of the impact of Kenenisa Bekele's cooperative drafting strategy on its running power during the 2019 Berlin marathon. *J. Biomech.* **107**, 109854 (doi:10.1016/j.jbiomech.2020.109854)
19. Schickhofer L, Hanson H. 2021 Aerodynamic effects and performance improvements of running in drafting formations. *J. Biomech.* **122**, 110457 (doi:10.1016/j.jbiomech.2021.110457)
20. Inoue T, Okayama T, Teraoka T, Maeno S, Hirata K. 2016 Wind-tunnel experiment on aerodynamic characteristics of a runner using a moving-belt system. *Cogent Eng.* **3**, 1231389 (doi:10.1080/23311916.2016.1231389)
21. Kyle C, Caiozzo V. 1986 The effect of athletic clothing aerodynamics upon running speed. *Med. Sci. Sports Exerc.* **18**, 509–515. (doi:10.1249/00005768-198610000-00003)
22. Blocken B, van Druenen T, Toparlar Y, Malizia F, Mannion P, Andrianne T, Marchal T, Maas G, Diepens J. 2018 Aerodynamic drag in cycling pelotons: new insights by CFD simulation and wind tunnel testing. *J. Wind Eng. Ind. Aerod.* **179**, 319–337. (doi:10.1016/j.jweia.2018.06.011)
23. Pugh LGCE. 1970 Oxygen intake in track and treadmill running with observations on the effect of air resistance. *J. Physiol.* **207**, 823–835. (doi:10.1113/jphysiol.1970.sp009097)
24. Pugh L. 1971 The influence of wind resistance in running and walking and the mechanical efficiency of work against horizontal or vertical forces. *J. Physiol.* **213**, 255–276. (doi:10.1113/jphysiol.1971.sp009381)
25. da Silva ES, Kram R, Hoogkamer W. 2022 The metabolic cost of emulated aerodynamic drag forces in marathon running. *J. Appl. Physiol.* **133**, 766–776. (doi:10.1152/japplphysiol.00086.2022)
26. Kipp S, Kram R, Hoogkamer W. 2019 Extrapolating metabolic savings in running: implications for performance predictions. *Front. Physiol.* **10**, 79 (doi:10.3389/fphys.2019.00079)
27. Beves C, Ferguson S. 2017 Uncovering the Aerodynamic Trickery Behind Nike's Breaking 2 Project (Online). See www.linkedin.com/pulse/uncovering-aerodynamic-trickery-behind-nikes-breaking-ferguson/ (accessed 4 July 2023).
28. TU/e. 2019 TU/e wind tunnel helped break the marathon's two-hour barrier (Online). See www.tue.nl/en/news/news-overview/12-10-2019-tue-wind-tunnel-helped-break-the-marathons-two-hour-barrier/ (accessed 3 May 2022).
29. Blocken B. 2019 Eliud Kipchoge Just Broke the Marathon's Two-Hour Barrier, and KU Leuven Research Helped Him Do It (Online). See https://nieuws.kuleuven.be/en/content/2019/ku-leuven-and-tu-eindhoven-helped-to-break-the-marathons-two-hour-barrier (accessed 4 July 2023).
30. Hill AV. 1928 The air-resistance to a runner. *Proc. R. Soc. Lond. B* **102**, 380–385. (doi:10.1098/rspb.1928.0012ISTEX)
31. Davies C. 1980 Effects of wind assistance and resistance on the forward motion of a runner. *J. Appl. Physiol.* **48**, 702–709. (doi:10.1152/jappl.1980.48.4.702)

32. Joint Committee for Guides in Metrology. 2008 JCGM 100: Evaluation of Measurement Data - Guide to the Expression of Uncertainty in Measurement. Technical report JCGM.
33. Pope S. 2000 *Turbulent flows*. Cambridge, UK: Cambridge University Press.
34. Achenbach E. 1971 Influence of surface roughness on the cross-flow around a circular cylinder. *J. Fluid Mech.* **46**, 321–335. (doi:10.1017/S0022112071000569ISTEX)
35. Wang HF, Zhou Y, Mi J. 2012 Effects of aspect ratio on the drag of a wall-mounted finite-length cylinder in the subcritical and critical regimes. *Exp. Fluids* **53**, 423–436. (doi:10.1007/s00348-012-1299)
36. Uematsu Y, Yamada M. 1995 Effects of aspect ratio and surface roughness on the time-averaged aerodynamic forces on cantilevered circular cylinders at high Reynolds numbers. *J. Wind Eng. Ind. Aerod.* **54–55**, 301–312. (doi:10.1016/0167-6105(94)00049)
37. Pankhurst RC. 1972 Aerodynamics at NPL, 1917–1970. *Nature* **238**, 375–380. (doi:10.1038/238375a0)
38. Hoogkamer W, Kram R, Arellano CJ. 2017 How biomechanical improvements in running economy could break the 2-hour marathon barrier. *Sports Med.* **47**, 1739–1750. (doi:10.1152/japplphysiol.00086.2022)
39. Marro M, Leckert J, Rollier E, Salizzoni P, Bailly C. 2023 Wind tunnel evaluation of novel drafting formations for an elite marathon runner. Figshare. (doi:10.6084/m9.figshare.c.6761804)